

Induction of T cell memory by a dendritic cell vaccine: a computational model

Francesco Pappalardo^{1*}†, Marzio Pennisi^{2†}, Alessia Ricupito³, Francesco Topputo⁴ and Matteo Bellone⁵

¹Department of Drug Science, University of Catania, Italy.

²Department of Mathematics and Computer Science, University of Catania, Italy.

³San Raffaele Scientific Institute and Università Vita Salute San Raffaele, Milan, Italy.

⁴Politecnico di Milano, Italy.

⁵San Raffaele Scientific Institute, Milan, Italy

Associate Editor: Dr. Ziv Bar-Joseph

ABSTRACT

Motivation: While results from phase III clinical trials substantially support the use of prophylactic and therapeutic vaccines against cancer, what has yet to be defined is how many and how frequent boosts are needed to sustain a long lasting and protecting memory T cell response against tumor antigens. Common experience is that such preclinical tests require the sacrifice of a relatively large number of animals, and are particularly time and money consuming.

Results: As a first step to overcome these hurdles, we have developed an ordinary differential equation model that includes all relevant entities (such as activated cytotoxic T lymphocytes and memory T cells), and investigated the induction of immunological memory in the context of wild type mice injected with a dendritic cell-based vaccine. We have simulated the biological behavior both in the presence and in the absence of memory T cells. Comparing results of ex vivo and in silico experiments, we show that the model is able to envisage the expansion and persistence of antigen-specific memory T cells. The model might be applicable to more complex vaccination schedules and substantially in any biological condition of prime-boosting.

Availability: The model is fully described in the article.

Contact: fp@francescopappalardo.net

1 INTRODUCTION

In the last years both therapeutic and preventive vaccines have been developed with the aim to fight and prevent different types of cancers (Kantoff, 2010; Kenter *et al.*, 2009; Kahn, 2009). The power of vaccines relies on their ability to stimulate a strong and long-lasting antigen-specific immune response, mediated both by B and T lymphocytes. While induction of a protective titer of neutralizing antibodies is the main objective of most of the vaccines against infectious agents, including vaccines to carcinogenic human papillomavirus (HPV) and hepatitis B virus (HBV), which also protect from cervical and liver cancer, respectively (Lollini *et al.*,

2011), evidence in humans that antibodies induced by a vaccine can contribute to antitumor immunity is scanty (Schoenfeld *et al.*, 2010). Conversely, the major goal of both prophylactic and therapeutic vaccines against non-infectious tumors, which account for approximately 80% of all tumors (Lollini *et al.*, 2011), is to induce a long-lasting antigen-specific CD8 T cell immunity. In support of this concept, high densities of effector memory CD8⁺ cytotoxic T cells are associated with a longer overall survival in several human cancers (Fridman *et al.*, 2012).

Usually, an effective vaccine, requires multiple immunizations in the form of prime-boost. Several studies have shown that boosting with a different vector carrying the same antigen is better at enhancing immune responses than boosting with the homologous vector. The mechanism underlying this phenomenon is still obscure. Heterologous prime-boost approaches are now widely used in efforts to develop vaccines (Kaufmann, 2010; Sallusto *et al.*, 2010). It is also generally accepted that a strong primary immune response is required to give rise to a large pool of memory cells (Sprent and Surh, 2011). However, what affects the longevity of memory T cells is not full understood, and much controversy exists regarding the role of antigens in this process (Zinkernagel, 2002; Sprent and Surh, 2011; Kaech *et al.*, 2002). Indeed, sustained high amounts of soluble antigens often lead to tolerance or exhaustion both in T and B cells. As a result of exhaustion, antigen-specific T and B cells express a variety of inhibitory receptors such as PD-1, LAG-3, CD244, CD160, TIM-3 and CTLA-4 (Wherry, 2011).

Dendritic cell (DC)-based vaccines have been extensively investigated as potential cancer therapeutic vaccines because of the primary role of DCs as antigen presenting cells (APCs) and their unique ability in T cell priming (Banchereau and Steinman, 1998). Indeed, DCs pulsed with the antigen of choice induce a potent antigen-specific immune response and favor the generation of the memory pool. This stems from the asymmetric division of engaged naive T cells into effector and memory cells (Chang *et al.*, 2007). Several phase II clinical trials based on the use of DCs pulsed with tumor associated antigens are ongoing (Finn, 2008). Moreover, Sipuleucel-T (Provenge; Dendreon, Inc.), an autologous APC-based vaccine has been the first vaccine approved by the Food and Drug Administration for the treatment of cancer patients. In

*To whom correspondence should be addressed.

†These authors equally contributed to this work.

a phase III trial in patients affected by castration-resistant prostate cancer Sipuleucel-T gave a 4.1-month benefit in overall survival relative to a control arm that received unpulsed APCs. However, no significant effects on the time to objective disease progression were observed (Kantoff, 2010). These promising results also suggest that some fundamental biological questions remain unanswered. Indeed, for DC-based vaccines it is not yet known whether booster immunizations should consist of DCs or other means. It has been reported that antigen-bearing DCs are rapidly eliminated by antigen-specific cytotoxic T lymphocytes (CTLs) when injected in previously vaccinated mice (Yang *et al.*, 2006; Guarda *et al.*, 2007), therefore arguing for a reduced effectiveness of DC-based boosts. Jouanneau et colleagues observed in the GL26 model that DCs are essential for the priming, but they are less effective than tumor cell lysate alone in boosting the anti-tumor immune response and for the induction of long-term immune memory (Jouanneau *et al.*, 2006). Another unsolved issue is the frequency of boosting. Indeed, it has been reported that repeated immunizations result in increased frequencies of memory T cells (Masopust *et al.*, 2006; Wirth *et al.*, 2010). However, over stimulation can drive memory T cells toward terminal differentiation such as activation-induced cell death, fratricide, or exhaustion (Overwijk and Restifo, 2001; Wherry, 2011).

To address these biological issues, we started analyzing the ability of DC-based vaccines to induce a long-lasting antigen specific immune response in mice. As immunological readout of antigen-primed and functional T cells, we measured the interferon gamma (IFN- γ) contained in sera of vaccinated mice, and the frequency of CD8⁺CD44⁺ T cells able to release IFN- γ upon *ex vivo* specific antigen challenge (Camporeale *et al.*, 2003). Preliminary experiments suggested that to optimize the best boosting strategy we would have had to set many experiments each lasting several months. To investigate these biological problems, as a first step, we began by setting up an *in silico* model capable to describe the biological phenomena observed in the animal model. The aim of the model is to verify the memory T cell induction hypothesis by a DC-based vaccine observed *in vivo*, and to give new suggestions on the designing of boosting strategies. During the last decades, several approaches have been devoted to model the immune system or parts of it, with mathematical equation-based models representing the largest slice among these approaches. Differential equation based models usually reproduce the dynamics of the average concentrations of the immune system involved entities over time, to obtain the main aspects of the immune response. Simple models based on systems of ordinary or partial differential equations can be easily analyzed to obtain, for example, asymptotic behaviors. On the other hand, for more complex scenarios, is usually difficult to build complex ordinary differential equations (ODE) based models as well as incorporate new aspects. The trade-off between an accurate biological representation and the mathematical feasibility may lead to biologically useless models or to mathematically intractable models.

Cellular automata (CA) or agent-based models (ABM) represent a large class of discrete modeling techniques where each entity is followed individually, and global behaviors are obtained from local behaviors of all involved entities. In this way it is possible to model the immune system in much more details, allowing to determine behaviour distribution (and not just the average). Moreover it is very easy to add and remove new entities and nonlinear interactions,

in order to expand or update the model to the last biological insights, leaving the problem computationally tractable. CA and ABM can be successfully used to simulate without any problems the receptor diversity of the immune repertoire, opening the door to natural scale simulations. An example of approaches in this direction are discussed in (Halling-Brown *et al.*, 2010). However, even such approaches have their own flaws: due to the lack of a solid mathematical theory, they miss tools allowing any asymptotic analysis, and require considerable computational power to simulate individual agents, in particular for large scale simulations. Some good review articles that can introduce the reader to the modeling techniques of the immune system are presented in (Perelson and Weisbuch, 1997; Lundegaard *et al.*, 2007; Germain *et al.*, 2011).

The problem we are dealing with requires the ability to uniquely represent the immune response of CTLs specific for the immunodominant Tag-IV antigen from the oncovirus SV40 (Mylin *et al.*, 1995), (and also *in vivo* measurements refer to this). This is a valid argument for supporting the assumption that a monoclonal model based on ODE described in this paper can be considered adequate. The (ODE) model includes all the relevant entities (such as activated CTLs and memory T cells) needed to confirm the presence of immunological memory. We simulated the biological behavior in the presence and in the absence of memory T cells.

2 METHODS

2.1 Model description

In order to model antigen-specific CTL activation and differentiation into memory T cells upon vaccination with pulsed DCs, we developed a model based on a system of 6 ODEs for 6 different populations: pulsed DCs (D_i) in the injection point, pulsed DCs (D_p) in the presenting locations, naive CTLs (T_n), activated CTLs (T_a), memory T cells (T_m) and IFN- γ (I).

Equations 1 and 2 deal with the pulsed DCs at the injection point and the presenting location, respectively. These two equations are used to model the injection of pulsed DCs into the host and their consecutive migration from the injection point to the site where presentation to CTLs occurs (i.e. lymph nodes). D_i (eqn. 1) are injected according to the function $k_{in}(t, q)$ that introduces into the system q pulsed DCs if, according to the administration protocol, at time t an injection is scheduled. D_i then migrate to presenting locations (term $-\alpha_{50}D_i$). They can also disappear from natural death (term $-\alpha_1D_i$).

$$\frac{dD_i}{dt} = k_{in}(t, q) - \alpha_{50}D_i - \alpha_1D_i \quad (1)$$

Equation 2 models the behavior of pulsed DCs into the presenting location. D_p are estimated on the basis of migrating D_i (term $\alpha_{50}D_i$) and disappear from the system for multiple causes, such as natural death (term $-\alpha_1D_p$).

$$\frac{dD_p}{dt} = \alpha_{50}D_i - \alpha_1D_p \quad (2)$$

We initially considered the possibility to model the migration process using delay differential equations, by adding in eqn 2 (term $\alpha_{50}D_i$) a time delay of approximately 2-4 hours. However, we abandoned this approach because after some numerical simulations we noted only negligible differences between results obtained with and without time delay. This is probably due to the fact that such a short time delay becomes insignificant in respect to the time-scale of the experiment (1 year).

Equation 3 models the antigen-specific naive CTLs behavior (T_n). In general when naive CTLs are activated, they are replaced by means of

haematopoiesis to keep the naive CTLs number almost constant as specified in the leukocyte formula. Of course, this does not mean that the newborn CTLs will share the same MHC/antigen complex specificity of previously activated cells. Present immunological knowledge cannot predict if and when a CTL will be replaced by one of the same specificity. Moreover, cells receptors are randomly selected by DNA recombinations. Hence, it is feasible to suppose that after a reasonable time window, the level of antigen-specific CTLs will approach to the same initial level. Finally, this is in line with the fact that the immunological repertoire is almost specific for each individual.

The term $h_1(T_{n0} - T_n)$ represents the recovery rate. Under safe conditions (absence of the pathogen) the number of T cells tends to a given value T_{n0} . When antigenic presentation by D_p occurs naive T cells are activated (term $-\alpha_5 D_p T_n$). We note here that equation 3 takes into account only a small portion of naive T cells population composed by those cells whose receptor is able to recognize the specific antigen, and not the entire T cells population.

$$\frac{dT_n}{dt} = h_1(T_{n0} - T_n) - \alpha_5 D_p T_n \quad (3)$$

Activated CTLs (T_a) are modeled by equation 4. They appear in the system as a consequence of the antigenic presentation to T_n by D_p cells (term $-\alpha_5 D_p T_n$) and can disappear from the system due to death ($-a_3 T_a$). As a consequence of activation, a small portion of activated T cells can become memory cells ($-a_{20} T_a$).

$$\frac{dT_a}{dt} = \alpha_5 D_p T_n - a_{20} T_a - a_3 T_a \quad (4)$$

Memory CTLs (eqn. 5) are estimated on the basis of activated T cells (term $a_{20} T_a$) and then disappear from the model due to multiple causes, among which natural death ($-a_{21} T_m$).

$$\frac{dT_m}{dt} = a_{20} T_a - a_{21} T_m \quad (5)$$

The last equation (eqn. 6) describes IFN- γ dynamics. The quantity of IFN- γ released by CTLs is taken as outcome of the ex vivo experiment and it is used to estimate the number of activated T cells. In order to compare our results with ex vivo observation we modeled IFN- γ dynamics as follows. IFN- γ is released by activated and memory T cells, which are supposed to release the same quantity of IFN- γ (term $h_{10}(T_a + T_m)$), and disappear from the model for natural degradation (term $-\alpha_{10} I$).

$$\frac{dI}{dt} = h_{10}(T_a + T_m) - \alpha_{10} I \quad (6)$$

It is worth mentioning here that the capacity to endow the host with the ability to learn through multiple encounters, and then generate memory, is in general not representable by ODEs. This important aspect has been analyzed using, for example, agent based modeling (Palladini *et al.*, 2010; Pennisi *et al.*, 2010). We modeled the learning phase that arises from the multiple encounters of T cells with targets cells by coding that into coefficients that were tuned in order to reproduce the fraction of memory T cells generated and observed in the mouse: the memory is then represented as the activation of dormant pathways.

Parameter values are shown in Table 1 and have been set at reasonable values based on results coming from the literature, from the observation of the in vivo experiments and from our past experience (Pappalardo *et al.*, 2009b; Pennisi *et al.*, 2008; Halling-Brown *et al.*, 2010; Pappalardo *et al.*, 2010; Pennisi *et al.*, 2009; Castiglione *et al.*, 2012; Pappalardo *et al.*, 2011, 2012, 2006, 2009a).

Numerical simulations start at week 8 ($t_0 = 0$), time of the first injection of pulsed DCs. The time-length of the simulations has been set to 360 days. The physical time step for the simulations is $\Delta(t) = 1$ day. To solve numerically the ODE system we used Berkeley Madonna software. Initial conditions have been set to 0 for all populations except for T_n where $T_n(0) = T_{n0}$. Since Tag-IV is an antigen specifically designed to give rise

Table 1. ODE model parameters. q represents the number of injected pulsed DCs / ml; it was tuned with in vivo results. a_1 is the pulsed DCs death rate (half-life ~ 7 days) (Merad and Manz, 2009). a_{50} is the migration rate of Di towards presentation location; it was tuned. h_1 is the T naive cells recover rate; it was tuned. a_5 is the CTL activation rate; it was tuned. a_3 is the activated T cell death rate (half-life ~ 2 days) (DeBoer *et al.*, 2003). a_{20} is the memory T cell differentiation rate; it was tuned. a_{21} is the memory T cell death rate (half-life 8 weeks); it was tuned. h_{10} is the IFN- γ quantity released by T cells (fg/ml) (Pennisi *et al.*, 2010). a_{10} is the IFN- γ degradation rate (half-life ~ 9 hours).

par.	value
q	500
a_1	$\ln(2)/7$
a_{50}	0.15
h_1	0.015
a_5	0.005
a_3	$\ln(2)/1.7$
a_{20}	0.03
a_{21}	$\ln(2)/10$
h_{10}	30
a_{10}	$\ln(2)/0.375$

to a very strong immune response, we supposed that approximately 20% of the total population of naive CTLs was potentially able to recognize the antigen. Supposing a total population of approximately 400 naive CD8 T cells per mm^3 , we set up $T_{n0} = 80$. The differentiation rate of activated CTLs (a_{20}) has been tuned up in such a way that the total number of newborn memory T cells for each injection of pulsed DCs is approximately around the 5% of the maximum number of activated T cells for each injection. Moreover to simulate lack of memory a_{20} has been set to 0. The parameters that we defined as "tuned" are free parameters, i.e. they were set in order to fit the experimental data. We highlight here that for these parameters there are no measures in the literature.

It's worth noting that we used the levels and the proportions of IFN- γ^+ cells and K^b/Tag^+ cells at week 9 to calibrate the model and the same levels and proportions at week 18 to validate the model results.

2.2 LHS-PRCC sensitivity Analysis

In order to understand which parameter may be considered fundamental in this process, it is important to analyze the sensitivity of the model to variation of parameters. Classical sensitivity analysis is usually done by varying a given parameter in reasonable ranges and keeping the others constant. Obviously results coming from this kind of analysis are strongly bound to the values of the fixed parameters and different sets of values for the fixed parameters may lead to completely different results.

Partial rank correlated coefficients (PRCC) (Saltelli, 2004) is a statistical sensitivity analysis technique which tries to overcome the limits of classical sensitivity analysis by computing a partial correlation on rank-transformed data between two sets of variables, represented in our case by the model input parameters and the model entities values. The strength of such a methodology is given by the fact that correlation does not depend by a given set of parameters, and it is therefore possible to estimate how variations in a given parameter may influence the results of the model, despite the value of the other parameters. Nevertheless the methodology can be in principle easily applied and used with any kind of continuous or discrete model.

The methodology we used to perform sensitivity analysis (LHS-PRCC) is briefly described as follows. More information about this methodology can be found in (Marino *et al.*, 2008). Parameters space is initially sampled

using a Monte-Carlo technique. In this case we use a technique named Latin-Hypercube-Sampling (LHS) (Mckay *et al.*, 1979). The technique divides the random parameter distributions into N (where N represents the chosen sample size) equal probability intervals that are then sampled. The choice for N should be at least $k + 1$, where k is the number of parameters varied, but usually much larger to ensure accuracy. In our trials we set $N = 1000$.

After sampling, a LHS matrix X of sampled parameters is built. Each row represents an unique set of variables for the model sampled without replacement.

The model is then solved for each row of X , and the model output values are stored into an output matrix Y . Each matrix is then rank-transformed (X_R and Y_R). X and Y can be used to calculate the Pearson correlation coefficient. X_R and Y_R can be used to calculate the Spearman or rank correlation coefficient (RCC) and the partial rank correlation coefficient (PRCC).

PRCC between an input parameter $x_j \in X_R$, $j \leq k$ and output $y \in Y_R$ is then computed by considering the residuals $x_j - \hat{x}_j$ and $y - \hat{y}$, where \hat{x}_j and \hat{y} are given by the following regression models:

$$\hat{x}_j = c_0 + \sum_{p=1, p \neq j}^k c_p x_p \quad \text{and} \quad \hat{y} = b_0 + \sum_{p=1, p \neq j}^k b_p x_p$$

Using this methodology we analyzed the effects of the most important input parameters which most influence the behaviour of the released IFN- γ . We plotted for these entities the PRCCs over the entire time course of the experiment to see how the sensitivity of parameters changes as system dynamics progresses and we showed the relative PRCC scatter plots at critical time-points. Results are available in Supplementary Data S1.

2.3 Mice and reagents

C57BL/6 mice were purchased from Charles River Italia (Calco, Italy). Animals were treated in accordance with the European Community guidelines and with the approval of the Institutional Ethical Committee. Unless specified, all chemical reagents were from Sigma-Aldrich, and monoclonal antibodies (mAb) were from BD Pharmingen.

2.4 DC preparation

DCs were prepared and characterized as previously described (Camporeale *et al.*, 2003). Briefly, bone marrow cells were seeded into six-well plates in ISCOVE supplemented with penicillin/ streptomycin and 10% foetal calf serum (Euroclone, Wetherby, UK), and the growth factors GM-CSF (25 ng/ml), and IL-4 (5 ng/ml; R&D Systems, Minneapolis, MN). Eight hours before retrieval of cells, the pro-maturation factor lipopolysaccharide (1 μ g/ml) was added to the culture medium. On day 7 of the *in vitro* culture, non-adherent and loosely adherent cells were collected. Culture supernatants were evaluated for Mycoplasma contamination by PCR, and positive cultures were discarded.

2.5 Immunization protocol

DCs were resuspended in phosphate buffered saline (PBS) at 2×10^6 /ml and pulsed with 2 μ M of the immunodominant CTL epitope Tag-IV peptide (VVYDFLKC; Research Genetics, Huntsville, AL) for 1 h at 37 Celsius, washed, resuspended in PBS, and subsequently injected intradermally (i.d.) into the right flank of mice (5×10^5 DC/mouse).

2.6 Schedule of immunization

Eight week-old C57BL/6 mice were primed by i.d. injection of Tag-IV-pulsed DCs (DC-Tag). Four weeks later the primed mice were boosted with DC-Tag and this process was repeated every 6 weeks for additional two times. Animals were killed 7 days after the first vaccination or 6 weeks after each boost.

2.7 Flow cytometry analyses

Spleens were collected and processed to single cell suspension. Splenocytes were stained *ex vivo* with phycoerythrin-labeled K^b /Tag-IV pentamers

(ProImmune, Sarasota, FL) in combination with the indicated fluorochrome-labeled monoclonal antibodies, the Dump mixture of antibodies (i.e., CD4, CD19, CD11c, CD11b), the vitality marker To-PRO3, and assessed by flow cytometry. Alternatively, cells were cultured in the absence or in the presence of 2 μ M Tag-IV peptide for 24h, of which, the last 3 were in the presence of brefeldin A (5 μ g/ml). Cells were then surface stained with fluorochrome-conjugated anti-CD4, anti-CD8, anti-CD44, anti-CD62L monoclonal antibodies, fixed, and analyzed for IFN- γ intracellular cytokine staining (DeglInnocenti *et al.*, 2005). PMA/ionomycin was used as positive control. Dead cells were excluded by physical parameters. IFN- γ^+ cells were gated on CD8 $^+$ CD44 $^+$, viable cells. Cytokine production in the absence of stimulation was considered as background release and subtracted from values obtained by the specific peptides. In all experiments, cells were acquired on a BD FACS Canto[®].

2.8 Statistical analysis of *in vivo* experimental studies

Prism 5.0a software was implemented to conduct statistical analysis on data collected in *ex vivo* immunological assays. Comparison of data collected from the different experimental groups of mice (at least 5 mice/group) was conducted using the ANOVA, and NewmanKeuls or the two-tailed Students *t* test tests. Values were considered statically significant for $P < 0.05$.

2.9 Measurements for *in silico* setup

In order to set up the *in silico* approach we measured the induction and maintenance of an antigen-specific CTL response in C57BL/6 mice injected with DCs pulsed with Tag-IV, the immunodominant CTL epitope from the SV40 Tag antigen (DC-Tag) (Mylin *et al.*, 1995).

2.10 Ethics Statement

Wild type C57BL/6 mice (Charles River Breeding Laboratories; Calco, IT) were housed in a pathogen-free animal facility, and treated in accordance with the European Community guidelines. The *in vivo* experiments were approved by the Ethical Committee of the Istituto Scientifico San Raffaele (IACUC # 410).

3 RESULTS AND DISCUSSION

3.1 The biological experiment

Eight-week-old mice were primed with a single i.d. injection of DC-Tag, and a first group was sacrificed one week later (Figure 1A). A substantial amount of CD8 $^+$ CD44 $^+$ T cells were found in the spleen of vaccinated mice that bound K^b /Tag pentamers (Figure 1B), therefore demonstrating to be antigen-experienced and specific for Tag. Among the Tag-specific T cells, almost 80% displayed an effector phenotype (i.e. CD62L $^-$), whereas more than 20% were central memory (Figure 1C). We investigated if the IFN- γ measured in the sera of vaccinated mice could be used as an indicator of the effector function of antigen-specific CD8 $^+$ T cells. Indeed, the amount of IFN- γ in the sera of vaccinated mice one week after priming was more than 3-fold the amount found in naive littermates (56.3 ± 10.8 vs 17.2 ± 2.5 pg/ml, respectively). However, this value remained stable thereafter, and did not mimic the drop in Tag-specific T cells found by pentamer staining at week 18 (Figure 1B and data not shown). This was likely due to the fact that several cells of the innate and adaptive arms of the immune system concur in producing IFN- γ upon vaccination. Thus, we utilized an *ex vivo* intracellular production assay to investigate the effector function of antigen-specific T cells activated by vaccination. Interestingly, a fraction of CD8 $^+$ CD44 $^+$ T cells similar to that found with K^b pentamer staining (Figure 1B) also produced IFN- γ

upon antigen-specific challenge (Figure 1D) and specifically killed targets expressing the relevant antigen (data not shown), therefore confirming our previously published data (Rigamonti *et al.*, 2011). To investigate the effects of boosts on the dimension of the antigen-specific memory pool, mice were boosted with DC-Tag 4 weeks later. This time schedule was chosen based on the notion that an ideal memory CTL response requires 4-6 weeks to settle in (Sallusto *et al.*, 2010). In spite of the recent vaccination, one week after the first boost the percentage (Figure 1D) and number (Figure 1F) of $CD8^+CD44^+$ T cells producing $IFN-\gamma$ substantially decreased. Mice were boosted 6 weeks later, and the last group of mice was sacrificed 6 weeks after the third boost (Figure 1A). As expected from a memory response measured more than a month after immunization (Wirth *et al.*, 2010), the number of Tag-specific splenocytes dropped of almost one log (Figure 1B), whereas central memory T cells increased (Figure 1C). A similar proportion between effector and memory T cells was found within the population of $IFN-\gamma^+$ cells (Figure 1E), therefore suggesting that K^b/Tag and $IFN-\gamma$ stained the same cells. Interestingly, both the 1D) and the absolute number (Figure 1F) of antigen-specific CTL remained stable thereafter, therefore suggesting that the vaccination procedure allowed the induction of a long-lasting antigen-specific memory response.

3.2 The in silico experiment

In order to model CTL activation and differentiation into memory T cells upon vaccination with pulsed DCs, we developed a model based on a system of 6 ODEs for 6 different populations (for details see Materials and Methods section).

3.2.1 Supporting long last T memory hypothesis. In Figure 2 we show the ODE immune system behavior for the following entities: DC-Tag in the injection point and where the antigen is presented (D_i and D_p , respectively), naive, activated and memory antigen specific CTLs (T_n , T_a and T_m), and the levels of $IFN-\gamma$ released by antigen-specific CTLs (I), starting from week 8 for a period of one year. To compare ex vivo results with the in silico experiments, we evaluated the total number of activated and memory $CD8^+$ T cells and their percentage measured at week 9 and 18 (Figures 3 and 4). Figure 3 shows the total number of Tag^+ cells (both activated and memory specific CTLs) at weeks 9 and 18. Comparing these results with Figure 1B one can notice that the model qualitatively reproduces the same proportions observed ex-vivo. Moreover, looking at Figure 4 the percentage of specific memory CTLs follows the same dynamics observed ex-vivo in Figure 1C. These results are in good agreement with the ex vivo data, and all together support the immunological memory hypothesis.

3.2.2 Prediction of the role of the second injection (Boosting) over the pool of memory T cells. To both investigate the role of the second injection (boosting) over the pool of memory Tag-specific CTLs, and to verify the prediction capabilities of the mathematical model, we simulated two scenarios. In these simulations we executed, as in previous experiments, the first priming with Dc-Tag at week 8. This priming was followed (or not) by a second injection of Dc-Tag at week 12 (boost). The outcome of the experiment was represented by the number of specific CTLs ($T_a + T_m$) at week 9, and at week 18 both in presence and absence of the boosting. The

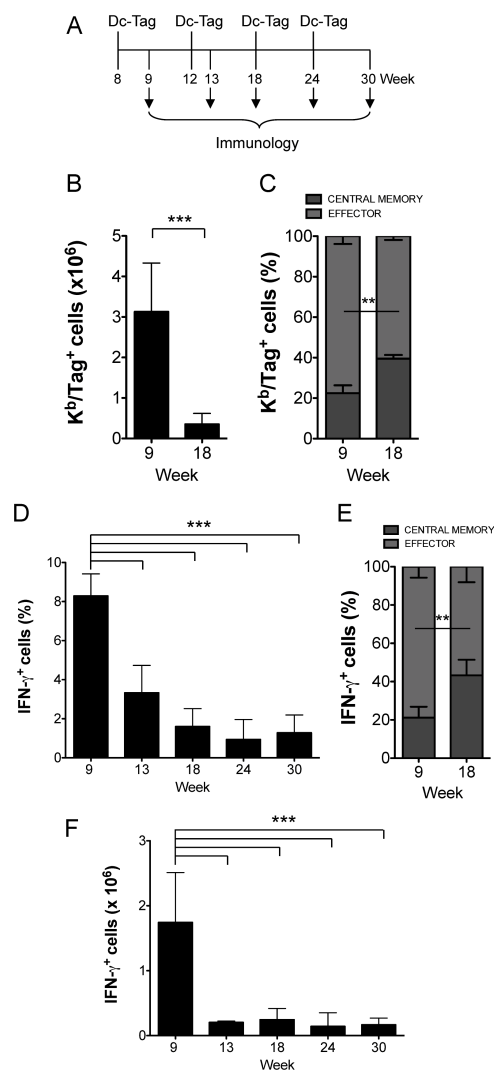


Fig. 1. Dynamics of antigen-specific $CD8^+$ T cells during the vaccination schedule. (A) Schematic representation of the experiment. Eight-week-old C57BL/6 mice were primed by i.d. injection of DC-Tag. Four weeks later, the mice were boosted with DC-Tag and this procedure was repeated twice every 6 weeks. Groups of animals were killed one week after the first injection of DC-Tag (week 9, $n=5$), one week after the first boost (week 13; $n=5$), or 6 weeks after each boost (week 18, $n=13$; week 24, $n=10$; and week 30, $n=9$). (B) Splenocytes from vaccinated mice were investigated for their specificity by staining with K^b/Tag pentamers. Data are reported as percentage \pm SD of K^b/Tag^+ cells within the gate of $CD8^+$ T cells. (C) Percentage of effector and central memory $CD8^+$ T cells within the K^b/Tag^+ cells. The effector function of Tag-specific $CD8^+$ T cells was assessed ex vivo by flow cytometry analysis of intracellular $IFN-\gamma$ production in the presence of Tag-IV. Percentage (D) and total number (F) of $IFN-\gamma$ -producing cells are depicted following electronic gating on $CD8^+ CD44^+$ viable cells. (E) Percentage of effector and central memory $CD8^+$ T cells within the $IFN-\gamma^+$ cells. Data are representative of at least 3 independent experiments. Statistical analyses were done using the ANOVA, and Newman-Keuls, and Student's t test tests. *** $p < 0.001$ and **: $0.001 < p < 0.01$.

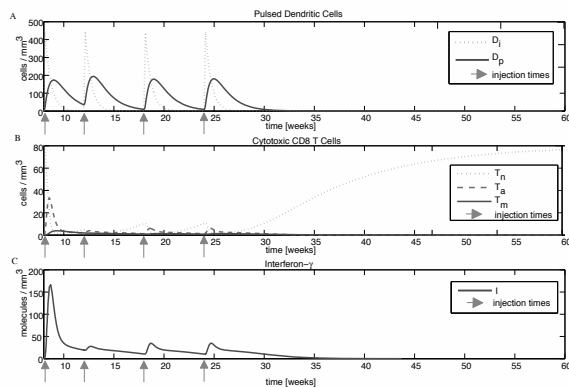


Fig. 2. ODE model dynamics. Dynamics for pulsed DCs, CD8 T cells and IFN- γ . (A) D_i represents the dynamics of injected DCs pulsed with the antigen, while D_p represents their dynamics in the presentation locations, i.e. lymphnodes. (B) T_n represents the dynamics of naive CTLs, T_a depicts the dynamics of activated CTLs, while T_m are the memory T cells. (C) Dynamics of IFN- γ released by antigen-specific CTLs (I).

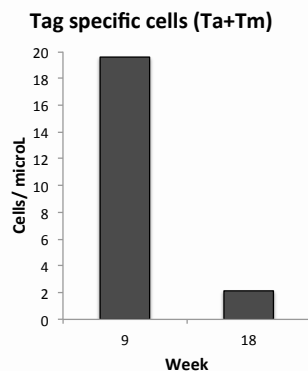


Fig. 3. Tag specific activated and memory CD8⁺ T cells. Tag specific activated and memory CD8⁺ T cells/mcl ($T_a + T_m$) measured in silico at week 9 and 18.

simulations showed a lower level of specific memory CTLs in the absence of the boosting (see Figure 5).

A similar experiment was then set-up in vivo, where the mice were primed at week 8 by DC-Tag. The initial set of mice was divided in three groups. The first group was sacrificed at week 9 (priming) to measure primary response. The second and third groups were left untouched (no boost) or boosted at week 12 with DC-Tag and sacrificed after an additional 6 weeks (week 18). As already showed by the mathematical model, the boosting had a substantial impact on the percentage of CD8⁺CD44⁺ CTLs producing IFN- γ (see Figure 5), and in vivo results reported the same behaviors (from a qualitative point of view) already observed with the mathematical simulations. The mathematical model demonstrated, was hence able to anticipate the importance of the second injection in promoting the generation of long-lived memory CTLs.

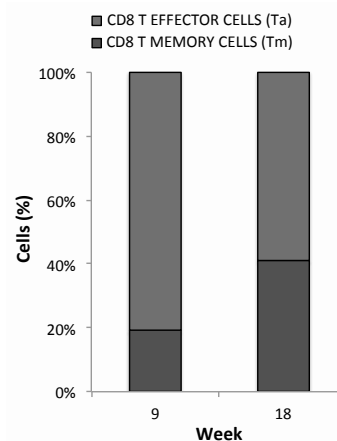


Fig. 4. Percentage of specific effector and memory CD8⁺ T cells. Percentage of specific effector and memory CD8⁺ T cells ($T_a + T_m$) measured in silico at week 9 and 18. Percentages are in a good agreement with the ex vivo results (see Figure 1C).

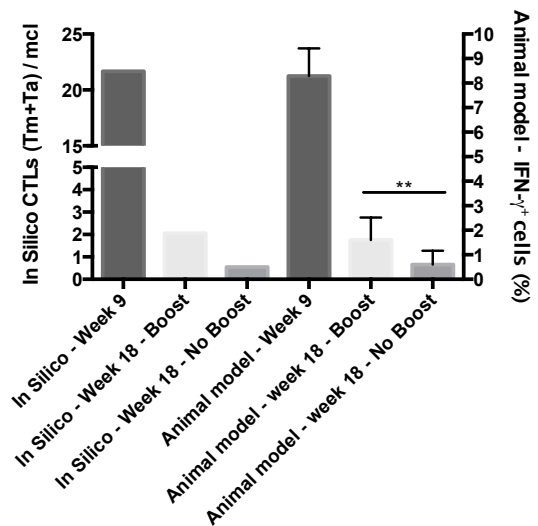


Fig. 5. Importance of the second injection over the pool of memory CTLs predicted by the mathematical model (in silico) and confirmed by the in vivo experiment (animal model). (A) Schematic representation of the experiment. Eight-week-old C57BL/6 mice were primed by i.d. injection of DC-Tag and either killed one week later (week 9, n=5) or boosted (Boost, n=13) or not (No Boost, n=13) 4 weeks later, and sacrificed 10 weeks after priming (week 18). (B) For the in silico experiment the number of specific memory CTLs ($T_m + T_a$) at week 9, and at week 18 both in presence and absence of the boosting were taken into account; For the in vivo experiments, the effector function of Tag-specific CD8⁺ T cells was assessed ex vivo by flow cytometry analysis of intracellular IFN- γ production in the presence of Tag-IV. Percentage of IFN- γ -producing cells are depicted following electronic gating on CD8⁺CD44⁺ viable cells. (Data are representative of at least 3 independent experiments. Statistical analyses were done using the Student's T test tests. **: 0.001 < p < 0.01).

3.3 LHS-PRCC Sensitivity analysis

Since activated CTLs release IFN- γ , we tracked, using partial rank correlation coefficient (PRCC) analysis, the effects of the model

parameters on the quantity of the released cytokine. It's worth mentioning here, that the results of the analysis we performed are strictly dependent on the 4-injections vaccination schedule we have modeled. Results of sensitivity analysis are available as Supplementary data S1. Here we only outline the major findings.

3.3.1 Role of CTL differentiation and death rates over $IFN-\gamma$. Sensitivity analysis reported that memory CTL differentiation rate coefficient a_{20} , which gives an estimation of the rate of activated CTLs (T_a) that differentiate into memory cells (T_m), showed a reduced correlation with $IFN-\gamma$, especially shortly after every DC-Tag, whereas such a correlation increased with the distance from the vaccine injection. This can be explained by the fact that after every injection, the immune response is mainly mediated by activated CTLs, whereas memory CTLs cells give a minor contribution at this time, especially after the first two injections. Far from injections, the immune response of activated CTLs declines and memory CTLs become the principal cells involved in $IFN-\gamma$ release. Similar considerations also hold when we verified the impact of memory CTL death rate on $IFN-\gamma$.

3.3.2 Role of naive CTL recovery rate over $IFN-\gamma$. The naive cell recovery rate (h_1), which refers to the speed at which the immune system reconstitutes the naive CTLs pool with newly generated CTLs, showed almost no correlation between the naive cell recovery rate and the $IFN-\gamma$ production, except for a short period of time around week 12, just after the second injection of DCs. At that time the number of T_n was lower than those related to the other administrations. It is worth noting that higher values of h_1 would entitle faster recruitment of specific naive CTLs and would allow higher levels of $IFN-\gamma$. However such a parameter cannot be modified in vivo. The presence of a positive PRCC correlation when the number of T_n is low may suggest that the second injection of vaccine is given too early, and it should be advisable to delay the second injection in order to give more time to the immune system to repopulate the specific naive CTLs population until no correlation is reached. Lack of correlation for the entire period may in fact represent an important achievement in designing a treatment that is effective not only for an individual, but for an entire population since small variations in the rate of recovery of naive cells for different individuals would not influence the efficacy of the treatment.

4 CONCLUSION

Our in silico model showed the ability to predict the dimension of the immune response induced in mice by DC vaccination, and allowed us to define the relative contribution of several parameters (i.e., memory cell differentiation and death rates and naive cell recovery rate) to the success of the prime-boost strategy. It also predicted the role of the second injection (Boost) over the pool of memory T cells. Nevertheless, it allowed the identification of a time window in which boosts may be detrimental (see Supplementary Data S1 for details). These findings appears to be consistent with data reported by us (Ricupito *et al.*, 2013a) and (Kaech *et al.*, 2002). We have demonstrated that boosting healthy mice every two weeks instead of every month hindered persistence of $IFN-\gamma$ -competent memory $CD8^+$ T cells (Ricupito *et al.*, 2013a). In addition, when vaccinated mice were challenged with melanoma

cells, 80% of the mice that had received a monthly boosting rejected the tumor. Conversely, mice treated with tighter vaccination schedules survived similarly to non boosted mice and remarkably less than mice boosted every month (Ricupito *et al.*, 2013b). One of the advantages of the system is that several entities and variables can be added each time. As an example, it might be interesting to investigate the role of endogenous DCs and the antigen formulation (e.g. synthetic peptide, protein or cell fragment) in T cell priming induced by the vaccine. It has been reported that the requirement of antigen transfer to endogenous APCs for in vivo CTL priming by DC-based vaccines may depend on the antigen formulation (Yewdall *et al.*, 2010). Furthermore, by adding the characteristic of the patient (e.g. age, sex, weight, general health status, stage of cancer, comorbidities, medications) a personalized vaccination schedule might be generated. One limit of the reported data is that they were obtained modeling a healthy subject, and therefore they are applicable only for the design of preventive vaccines. The system needs to be challenged against more stringent biological contexts such as in the presence of minimal residual disease or bulky tumors. Our recent findings suggest that tumor antigens released from the tumor as a consequence of either the tumor cell turnover or the immune attack already boost memory T cells induced by vaccine priming, and vaccine boosts may be detrimental. On the other hand, the model does not take into account the regulation of T cell longevity and the peculiarities of the antigens. These issues appear important and future version of the model could incorporate them, as wet experiments reveal their roles.

An additional limit of the study is that it is entirely based on mouse data. Indeed, there are no published clinical trials in which different vaccination schedules have been compared for induction of long-lasting antitumor immunity. Most of the vaccination protocols tested so far in cancer patients stemmed from the experience with prophylactic vaccines against infectious diseases, which are dissimilar to non-infectious tumors. Thus, reliable pre-clinical models are needed to investigate the therapeutic efficacy of cancer vaccines. Mice are the experimental tool of choice for the majority of tumor immunologists, because of the remarkable similarities between mouse and human immune system. Nevertheless, significant differences exist between mice and humans in immune system development, cell subpopulations of both the innate and adaptive arms, and perception of endogenous and exogenous activation signals (Mestas and Hughes, 2004). This should sound a word of caution to avoid over interpreting results obtained in mouse models.

Due to the fact that information is also available for humans on the 6 different populations we used to develop the related ODEs, our model might be easily tested in the human context, and provide useful information for DC-based cancer vaccines.

ACKNOWLEDGEMENT

We thank Dr. A. Napolitano (San Raffaele Scientific Institute, Milan, Italy) for technical suggestions. A.R. conducted this study as partial fulfillment of her PhD in Molecular Medicine, Program in Basic and Applied Immunology, San Raffaele University, Milan, Italy.

Funding: F.P. and M.P. acknowledge partial support from PRIN 2009, "Metodi e Modelli Matematici della Teoria Cinetica per

Systemi Complessi”. This study was supported by grants of the Italian Association for Cancer Research (AIRC, Milan) to M.B., the Ministry of Health (Rome) to M.B., the Ministry of University and Research (FIRB; Rome) to M.B.

REFERENCES

- Banchereau, J. and Steinman, R. (1998). Dendritic cells and the control of immunity. *Nature*, **392**(6673), 245–252.
- Camporeale, A., Boni, A., Iezzi, G., Degl’Innocenti, E., Grioni, M., Mondino, A., and Bellone, M. (2003). Critical impact of the kinetics of dendritic cells activation on the in vivo induction of tumor-specific T lymphocytes. *Cancer Res.*, **63**(13), 3688–3694.
- Castiglione, F., Motta, S., Pappalardo, F., and Pennisi, M. (2012). A modeling framework for immune-related diseases. *Mathematical Modelling of Natural Phenomena*, in press.
- Chang, J., Palanivel, V., Kinjyo, I., Schambach, F., Intlekofer, A., Banerjee, A., Longworth, S., Vinup, K., Mrass, P., Oliaro, J., Killeen, N., Orange, J., Russell, S., Weninger, W., and Reiner, S. (2007). Asymmetric T lymphocyte division in the initiation of adaptive immune responses. *Science*, **315**, 1687–1691.
- DeBoer, R., Homann, D., and Perelson, A. (2003). Different dynamics of CD4⁺ and CD8⁺ T cell responses during and after acute lymphocytic choriomeningitis virus infection. *J Immunol*, **171**(8), 3929–3935.
- Finn, O. (2008). Cancer Immunology. *N. Eng. J. Med.*, **358**(25), 2704–2715.
- Fridman, W., Pagès, F., Sautès-Fridman, C., and Galon, J. (2012). The immune contexture in human tumours: impact on clinical outcome. *Nat Rev Cancer*, **12**(4), 298–306.
- Germain, R. N., Meier-Schellersheim, M., Nita-Lazar, A., and Fraser, I. D. (2011). Systems biology in immunology: A computational modeling perspective. *Annual Review of Immunology*, **29**, 527–585.
- Guarda, G., Hons, M., Soriano, S., Huang, A., Polley, R., Martin-Fonoteca, A., Stein, J., Germain, R., Lanzavecchia, A., and Sallusto, F. (2007). L-selectin-negative CCR7- effector and memory CD8⁺ T cells enter reactive lymph nodes and kill dendritic cells. *Nat. Immunology*, **8**, 743–752.
- Halling-Brown, M., Pappalardo, F., Rapin, N., Zhang, P., Alemani, D., Emerson, A., Castiglione, F., Duroux, P., Pennisi, M., Miotto, O., Churchill, D., Rossi, E., Moss, D., Sansom, C., Bernaschi, M., Lefranc, M., Brunak, S., Lund, O., Motta, S., Lollini, P., Murgo, A., Palladini, A., Basford, K., Brusci, V., and Shepherd, A. (2010). Immunogrid: Towards agent-based simulations of the human immune system at a natural scale. *Philosophical Transactions of the Royal Society A: Mathematical, Physical and Engineering Sciences*, **368**(1920), 2799–2815.
- Jouanneau, E., Poujol, D., Gulia, S., Mercier, I. L., Blay, J., Belin, M., and Puisieux, I. (2006). Dendritic cells are essential for priming but inefficient for boosting antitumour immune response in an orthotopic murine glioma model. *Cancer Immunol. Immunother.*, **55**(3), 254–267.
- Kaech, S., Wherry, E., and Ahmed, R. (2002). Effector and memory T-cell differentiation: implications for vaccine development. *Nature Review Immunology*, **2**(4), 251–262.
- Kahn, J. (2009). HPV Vaccination for the Prevention of Cervical Intraepithelial Neoplasia. *The New England Journal of Medicine*, **361**, 271–278.
- Kantoff, P. (2010). Sipuleucel-T immunotherapy for castration-resistant prostate cancer. *N. Eng. J. Med.*, **363**(5), 411–422.
- Kaufmann, S. (2010). Future vaccination strategies against tuberculosis: thinking outside the box. *Immunity*, **33**(4), 567–577.
- Kenter, G., Welters, M., Valentijn, A., Lokw, M., van der Meer, D. B., Vloon, A., Essahsah, F., Fathers, L., Offringa, R., Drijfhout, J., Wafelman, A., Oostendorp, J., Fleuren, G., van der Burg, S., and Melief, C. (2009). Vaccination against HPV-16 Oncoproteins for Vulvar Intraepithelial Neoplasia. *The New England Journal of Medicine*, **361**(19), 1838–1847.
- Lollini, P., Nicoletti, G., Landuzzi, L., Cavallo, F., Forni, G., Giovanni, C. D., and Nanni, P. (2011). Vaccines and other immunological approaches for cancer immunoprevention. *Curr Drug Targets*, **13**, 1957–1973.
- Lundegaard, C., Lund, O., Kesmir, C., Brunak, S., and Nielsen, M. (2007). Modeling the adaptive immune system: predictions and simulations. *Bioinformatics*, **23**(24), 3265–3275.
- Marino, S., Hogue, I., Ray, C., and Kirschner, D. (2008). A Methodology For Performing Global Uncertainty and Sensitivity Analysis in Systems Biology. *Journal of Theoretical Biology*, **254**, 178–196.
- Masopust, D., Ha, S., Vezy, V., and Ahmed, R. (2006). Stimulation history dictates memory CD8 T cell phenotype: Implications for prime-boost vaccination. *J Immunol*, **177**, 831–839.
- Mckay, M., Beckman, R., and Conover, W. (1979). Comparison of 3 methods for selecting values of input variables in the analysis of output from a computer code. *Technometrics*, **21**(2), 239–245.
- Merad, M. and Manz, M. (2009). Dendritic cell homeostasis. *Blood*, **113**(15), 3418–3427.
- Mestas, J. and Hughes, C. (2004). Of mice and not men: differences between mouse and human immunology. *J Immunol*, **172**(5), 2731–2738.
- Mylin, L., Deckhut, A., Bonneau, R., Kierstead, T., Tevethia, M., Simmons, D., and Tevethia, S. (1995). Cytotoxic T lymphocyte escape variants, induced mutations, and synthetic peptides define a dominant H-2K^b-restricted determinant in simian virus 40 tumor antigen. *Virology*, **208**(1), 159–172.
- Overwijk, W. and Restifo, N. (2001). Creating therapeutic cancer vaccines: notes from the battlefield. *Trends Immunol*, **22**(1), 5–7.
- Palladini, A., Nicoletti, G., Pappalardo, F., Murgo, A., Grosso, V., Stivani, V., Ianzano, M. L., Antognoli, A., Croci, S., Landuzzi, L., Giovanni, C. D., Nanni, P., Motta, S., and Lollini, P. L. (2010). In silico modeling and in vivo efficacy of cancer-preventive vaccinations. *Cancer Research*, **70**(20), 7755–7763.
- Pappalardo, F., Mastriani, E., Lollini, P., and Motta, S. (2006). Genetic Algorithm against Cancer. *Lecture Notes in Computer Science*, **3849**, 223–228.
- Pappalardo, F., Motta, S., Cincotti, A., and Pennisi, M. (2009a). Agent based modeling of atherosclerosis: a concrete help in personalized treatments. *Lecture Notes in Computer Science*, **5755**, 386–396.
- Pappalardo, F., Halling-Brown, M., Rapin, N., Zhang, P., Alemani, D., Emerson, A., Paci, P., Duroux, P., Pennisi, M., Palladini, A., Miotto, O., Churchill, D., Rossi, E., Shepherd, A., Moss, D., Castiglione, F., Bernaschi, M., Lefranc, M., Bruna, S., Motta, S., Lollini, P., Basford, K., and Brusci, V. (2009b). ImmunoGrid, an integrative environment for large-scale simulation of the immune system for vaccine discovery, design and optimization. *Briefings in Bioinformatics*, **10**(3), 330–340.
- Pappalardo, F., Pennisi, M., Castiglione, F., and Motta, S. (2010). Vaccine protocols optimization: In silico experiences. *Biotechnology Advances*, **28**(1), 82–93.
- Pappalardo, F., Forero, I., Pennisi, M., Palazon, A., Melero, I., and Motta, S. (2011). SimB16: modeling induced immune system response against B16-melanoma. *PLoS ONE*, **6**(10): e26523, doi:10.1371/journal.pone.0026523.
- Pappalardo, F., Palladini, A., Pennisi, M., Castiglione, F., and Motta, S. (2012). Mathematical and computational models in tumor immunology. *Mathematical Modelling of Natural Phenomena*, **7**(3), 186–203.
- Pennisi, M., Catanuto, R., Pappalardo, F., and Motta, S. (2008). Optimal vaccination schedules using simulated annealing. *Bioinformatics*, **24**(15), 1740–1742.
- Pennisi, M., Pappalardo, F., Zhang, P., and Motta, S. (2009). Searching of optimal vaccination schedules. *IEEE Engineering in Medicine and Biology Magazine*, **28**(4), 67–72.
- Pennisi, M., Pappalardo, F., Palladini, A., Nicoletti, G., Nanni, P., Lollini, P. L., and Motta, S. (2010). Modeling the competition between lung metastases and the immune system using agents. *BMC Bioinformatics*, **11**(SUPPL. 7), doi:10.1186/1471-2105-11-S7-S13.
- Perelson, A. S. and Weisbuch, G. (1997). Immunology for physicists. *Reviews of Modern Physics*, **69**(4), 1219–1267.
- Ricupito, A., Grioni, M., Calcinotto, A., Michelini, R., Longhi, R., Mondino, A., and Bellone, M. (2013a). Booster Vaccinations against Cancer Are Critical in Prophylactic but Detrimental in Therapeutic Settings. *Cancer Research*, **73**, 3545–3554.
- Ricupito, A., Grioni, M., Calcinotto, A., and Bellone, M. (2013b). Boosting anticancer vaccines: Too much of a good thing? *Oncimmunology*, **2**(7), e25032.
- Rigamonti, N., Capuano, G., Ricupito, A., Jachetti, E., Grioni, M., Generoso, L., Freschi, M., and Bellone, M. (2011). Modulators of arginine metabolism do not impact on peripheral T-cell tolerance and disease progression in a model of spontaneous prostate cancer. *Clinical Cancer Research*, **17**(5), 1012–1023.
- Sallusto, F., Lanzavecchia, A., Araki, K., and Ahmed, R. (2010). From Vaccines to Memory and Back. *Immunity*, **33**(4), 451–463.
- Saltelli, A. (2004). *Sensitivity Analysis in Practice: A Guide to Assessing Scientific Models*. Wiley, Hoboken, NJ.
- Schoenfeld, J., Jinushi, M., Nakazaki, Y., Wiener, D., Park, J., Soiffer, R., Neuberger, D., Mihm, M., Hodi, F., and Dranoff, G. (2010). Active immunotherapy induces antibody responses that target tumor angiogenesis. *Cancer Research*, **15**(70(24)), 10150–60.
- Sprent, J. and Surh, C. (2011). Normal T cell homeostasis: the conversion of naive cells into memory-phenotype cells. *Nat. Immunology*, **12**(6), 478–484.
- Wherry, E. (2011). T cell exhaustion. *Nat. Immunology*, **12**(6), 492–496.
- Wirth, T., Harty, J., and Badovinac, V. (2010). Modulating numbers and phenotype of CD8⁺ T cells in secondary immune responses. *European Journal of Immunology*,

-
- 40(7), 1916–1926.
- Yang, J., Huck, S., McHugh, R., Hermans, I., and Ronchese, F. (2006). Perforin-dependent elimination of dendritic cells regulates the expansion of antigen-specific CD8⁺ T cells in vivo. *Proc. Natl. Acad. Sci. USA*, **103**, 147–152.
- Yewdall, A., Drutman, S., Jinwala, F., Bahjat, K., and Bhardwaj, N. (2010). CD8⁺ T Cell priming by dendritic cell vaccines requires antigen transfer to endogenous antigen presenting cells. *PLoS ONE*, **5**, e11144.
- Zinkernagel, R. (2002). On differences between immunity and immunological memory. *Curr. Opin. Immunol.*, **14**, 523–536.